J. Physiol. (1984), **354**, *pp.* 577–604
With 12 text-figures
Printed in Great Britain

RELAXATION OF RABBIT PSOAS MUSCLE FIBRES FROM RIGOR BY PHOTOCHEMICAL GENERATION OF ADENOSINE-5′-TRIPHOSPHATE

BY Y. E. GOLDMAN*, M. G. HIBBERD* AND D. R. TRENTHAM†

From the Department of Physiology and the Department of Biochemistry and Biophysics†, University of Pennsylvania, Philadelphia, PA 19104, U.S.A.*

(*Received 6 December 1983*)

SUMMARY

1. Correlations have been made between the mechanical and biochemical descriptions of muscle relaxation. Skinned muscle fibres in the rigor state were incubated in a solution containing P^3-1-(2-nitro)phenylethyladenosine-5′-triphosphate, 'caged ATP', an inert photolabile precursor of ATP, and free Ca^{2+} concentration $< 10^{-8}$ M. The mechanical response of the fibre was monitored during relaxation initiated by liberating ATP with a pulse of 347 nm light from a frequency-doubled ruby laser.

2. Tension first dropped and then rose briefly, before finally declining to the relaxed level. Stiffness, in phase with a sinusoidal length change, declined monotonically after the laser pulse. Out-of-phase stiffness increased briefly after a delay, then returned to the base line during the final relaxation. The development of the out-of-phase stiffness signal was taken as evidence that during the relaxation some cross-bridges were present with properties similar to those in an active contraction.

3. The tension rise and slower phase of relaxation can be explained by a mechanism in which some of the cross-bridges reattach, generate force and finally detach in the absence of Ca^{2+} ions. In this model cross-bridge attachment is facilitated by protein co-operativity within the myofilaments. Detailed analysis of the mechanical transients makes other possible models for the initial tension rise unlikely.

4. Stretching or releasing fibres prior to photolysis changed the time course of the early parts of the tension transient without significant effect on the later phases or on stiffness. The tension records from stretch, release and isometric trials converged to a final common time course of relaxation.

5. Analysis of the convergence of tension records provided a means for measuring the cross-bridge detachment rate from the thin filament as a function of ATP concentration. The apparent second-order rate constant for detachment was at least 5×10^5 M^{-1} s^{-1} at 20–22 °C. The final relaxation rate was less dependent on ATP concentration than the early convergence.

6. The results indicate that ATP binding and cross-bridge detachment from the nucleotide-free intermediate of the cross-bridge cycle are rapid compared to the cross-bridge cycling rate.

INTRODUCTION

It is a postulate of the cross-bridge hypothesis of muscle contraction that globular heads of myosin in the thick filaments of the sarcomeres cyclically attach to actin in the thin filaments, exert a relative sliding force between the filaments and then detach (A. F. Huxley, 1974, and references therein). Recently we have begun to obtain direct correlation between the mechanical and biochemical mechanisms of the cross-bridge cycle through a new photochemical technique. This method permits rapid liberation of ATP, ADP or P_i at known concentrations within a muscle fibre on a time scale that allows the mechanical response to be directly correlated with the nucleotide concentration. In this technique, a skinned muscle fibre (i.e. the sarcolemma is mechanically or chemically removed) is bathed in a solution containing 'caged ATP' (P^3-1-(2-nitro)phenylethyladenosine-5′-triphosphate), a biologically inert, but photolabile, precursor of ATP (Kaplan, Forbush & Hoffman, 1978). Following a pulse of near-ultraviolet radiation, ATP is liberated in the fibre and the mechanical response is monitored.

When muscle fibres are in rigor, photolysis of caged ATP in the absence of free Ca^{2+} ions causes tension and stiffness to decrease rapidly to the relaxed level (Goldman, Hibberd, McCray & Trentham, 1982*b*). The relaxation rate is rapid compared to the cross-bridge cycling rate, as judged from the rate of ATP splitting in actively contracting muscle. However, relaxation of rigor tension occurs about 5–10 times more slowly than the rate of ATP-induced acto-heavy meromyosin dissociation (White & Taylor, 1976).

Several factors could decrease the rate of relaxation in the photolysis experiment: (1) ATP is not released instantaneously on photolysis of caged ATP, but with a rate constant of approximately $100\ s^{-1}$; (2) since the myosin head concentration is substantial, the ATP concentration within the fibre declines as ATP binds to myosin; (3) reattachment of some detached cross-bridges before final relaxation would delay relaxation. The third possibility was suggested by a transient increase in tension observed when the initial rigor tension or the released ATP concentrations are low. However, factors other than reattachment might contribute to the transient rise in tension. Possible mechanisms include detachment of cross-bridges bearing a negative (compressive) force or generation of high force by an actomyosin.ATP state before detachment.

Experiments presented in this paper test the reattachment hypothesis by further characterization of the fibre's mechanical state following photolysis of caged ATP. A method is presented to isolate the rate of the first detachment of cross-bridges from subsequent events. An estimate is then made of the rate constant of ATP-induced detachment of rigor cross-bridges, taking into account the rate of ATP release on photolysis of caged ATP and also the effect of the finite myosin head concentration. In the following paper the mechanical response of muscle fibres is described when ATP is released in the presence of free calcium ions (Goldman, Hibberd & Trentham, 1984).

METHODS

Muscle fibre preparations

Muscle fibres were obtained from male or female New Zealand white rabbits (3–4 kg). The psoas muscle was exposed ventrally and a bundle of about 100 fibres was gently separated from the muscle. Single skinned fibres were prepared by one of two methods, each of which gave similar results.

In some cases fresh single (cut) fibres were dissected under silicone oil at ≈5–10 °C. The surface membrane was everted and then peeled off with an electrolytically sharpened tungsten needle as the fibre was drawn through a droplet of relaxing solution (Table 1) (Natori, 1954; Goldman & Simmons, 1984).

TABLE 1. Composition of solutions

A. Solutions used during caged ATP photolysis trials

	Mg ATP	$MgCl_2$	Mg^{2+}	EGTA	Ca^{2+}	$K^+ + Na^+$	TES	CP	CK†	GSH	Caged ATP
Rigor	0	3·2	1	53	*	140	100		0	10	0–10
Rigor with CP	0	2·6	1	30	*	138	100	22	1	10	0–10
0·1 mM-ATP relax	0·1	2·7	1	30	*	138	100	22	1	10	0
5·0 mM-ATP relax	5·0	7·4	1	30	*	141	100	11	0	10	0

B. Solutions used to prepare and store skinned fibres

	ATP	Mg^{2+}	EGTA	Ca^{2+}	Imidazole	KP	NaN_3	PMSF	Glycerol
Skinning solution	2·5	2·5	5	*	10	170	0	0·1	0
Storage solution	2·5	2·5	5	*	10	170	5	0	50 % (v/v)

* $Ca^{2+} < 10^{-8}$ M.

† mg ml^{-1} 100–150 units activity: 1 unit transfers 1·0 μmol phosphate from CP to ADP per minute at pH 7·4 and 30 °C (Sigma Chemical Co.).

All concentrations mM unless stated otherwise. Over-all ionic strength of the solutions was 0·2 M. Solutions in A were made up at room temperature (20–22 °C) and brought to pH 7·1 with KOH or HCl; solutions in B were brought to pH 7·0.

EGTA ethyleneglycol-*bis*-(β-aminoethylether)-*N*,*N*,*N*′,*N*′-tetraacetic acid.
TES *N*-Tris(hydroxymethyl)methyl-2-aminoethanesulphonic acid.
GSH glutathione (reduced form).
KP potassium propionate.
PMSF phenylmethylsulphonyl fluoride.
CP creatine phosphate.
CK creatine kinase.

Most experiments were performed on chemically skinned fibres prepared by a modification of the method described by Eastwood, Wood, Bock & Sorensen (1979). Thin bundles of fibres (1 mm in diameter; 2–3 cm long) were tied to wooden sticks and immersed for 2 h in a skinning solution (Table 1) at 0 °C with gentle agitation. Fibres were then transferred to fresh solution in airtight glass jars and agitated at 4 °C for 24 h. The fibres were finally transferred to a storage solution (Table 1), slowly cooled to −22 °C and stored for up to 3 months. Inclusion of phenylmethylsulphonyl fluoride (PMSF) and sodium azide in the skinning and storage solutions reduced deterioration of the fibres during storage.

Single-fibre segments were separated from the bundles under silicone oil and relaxed at 10–12 °C in 5 mM-Mg ATP. T-shaped aluminium foil clips made by a photolithographic process (Goldman & Simmons, 1984) were folded around each end of the fibre.

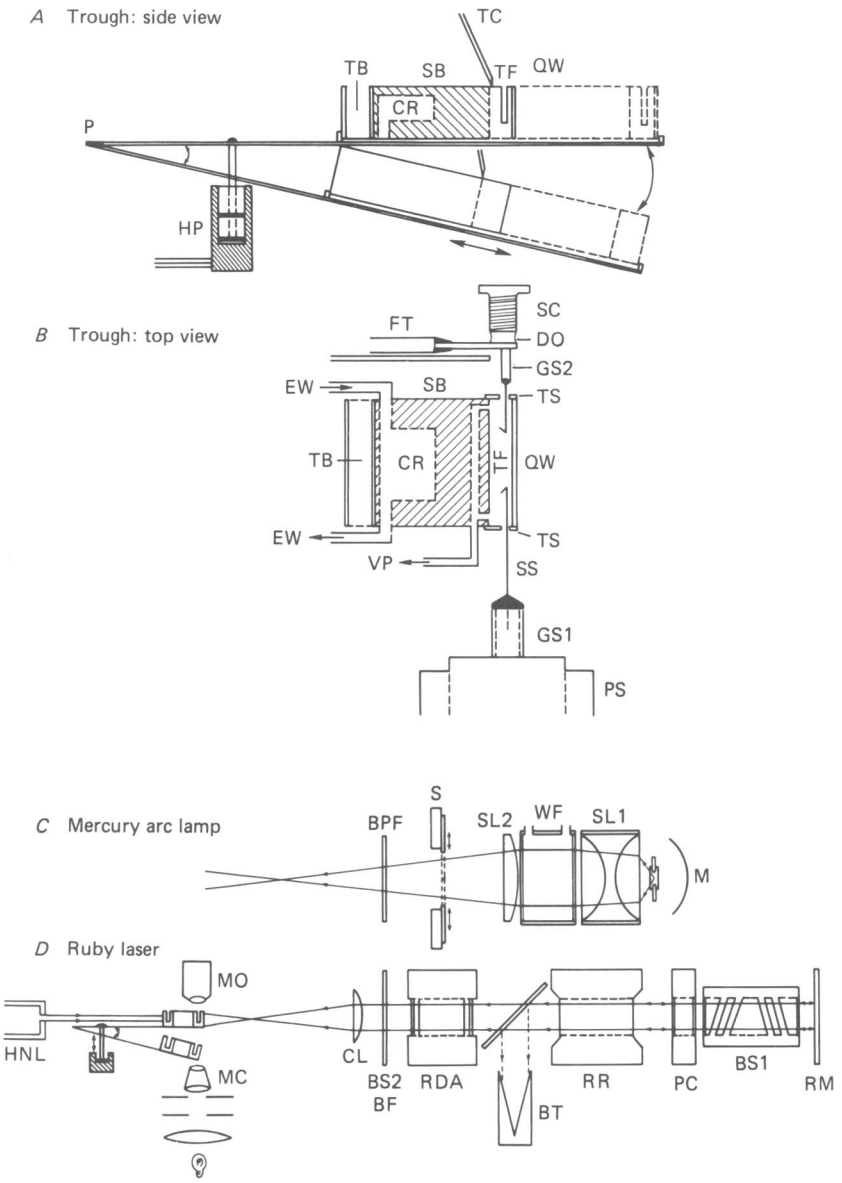

Fig. 1. Experimental apparatus used for laser flash photolysis of caged ATP within skinned muscle fibres. *A* **and** *B*, **side and plan views of the muscle troughs, force transducer and length controller assembly. Two troughs were built on opposite ends of a stainless-steel block (SB). The block contained a reservoir (CR) for circulating ethanol/water coolant (EW) and vacuum ports (VP) for emptying solutions from the front trough (TF). TF had a 0·5 mm thick quartz window (QW) nearest to the light sources, and Teflon side walls (TS) with vertical slots to allow access for connexions to the force transducer (FT) and piezoelectric length controller (PS). TF also had a glass floor to allow illumination for direct light microscopy. The back trough (TB) was constructed of Delrin. An automatically controlled hydraulic piston (HP) was used to raise and lower the trough assembly, which moved on a horizontal slide for solution exchange as indicated by the horizontal arrows. A Teflon cannula (TC) connected to a motorized syringe (not shown) delivered solutions**

Mechanical measurements

Fig. 1 illustrates the experimental set-up. Fibres were mounted horizontally in a trough filled with 20 μl relaxing solution (Fig. 1 *A*). The clips were attached to hooks on a force transducer (FT) and a ceramic piezoelectric stack (PS). Fibres were mounted slack and then extended 5–10 % by moving the piezoelectric device on a rack-and-pinion slide. Sarcomere lengths and fibre dimensions were determined by direct light microscopy as described in Goldman & Simmons (1984). The striation spacing in relaxing solution was 2·3–2·5 μm.

The piezoelectric element was obtained from Physike Instrumente, GmbH, model P-173. A hollow grass stem (GS1, 3 mm diameter), braced with thin parallel carbon fibre strips (kindly supplied by AERE, Harwell) and painted with epoxy resin, was fixed in-line with the moving part of the piezoelectric stack. A hardened stainless-steel hook was attached to the stem with heat-sensitive shellac, with facilitated alignment of the hook with the fibre axis. The piezoelectric stack was driven by command signals from a custom-built ramp generator and a high-voltage amplifier (Trek, model 609-5). The full range of movement of the piezoelectric stack was 40 μm, with 8 % non-linearity over the 24 μm range used in the experiments. A step change of position was complete within 800 μs. Sinusoidal length commands (0·5–2·5 kHz) from a wave-form generator (Wavetek, model 166) or from a lock-in amplifier (Ithaco, model 393) were added to the steady length command.

Fibre tension was detected by a silicon-beam strain gauge (Akers, Horten, Norway, model AE 801) mounted as described by Goldman & Simmons (1984). The over-all sensitivity of the transducer system was about 500 mV/mN with noise of 4 μN peak-to-peak, at band width 10 kHz. Drift was negligible during experiments. Damping of the strain-gauge resonance was accomplished by placing a small drop of gear oil (Fig. 1 *B*; DO, Castrol, Hypoy) between the rear surface of the element and the flat front surface of a finely threaded adjustment screw (SC, Fig. 1 *B*). The natural frequency of the transducer and connexions was 5 kHz.

The tension signals consisted of steady or transient muscle fibre force and a small (<5 %) superimposed sinusoidal force component due to the length oscillation applied by the piezoelectric device. The in-phase sinusoidal component of tension is approximately proportional to the high-frequency stiffness of the muscle fibre. The (90 deg) out-of-phase component or 'quadrature stiffness' is related to viscosity or viscoelasticity. These two sinusoidal components were separated from the steady component of muscle fibre tension by synchronous demodulation (Schwartz, 1959) and low-pass filtering. The initial experiments were conducted using an Evans model 4110 demodulator and low-pass filter for detection of the in-phase stiffness. In later experiments a lock-in amplifier (Ithaco, model 393) was used to demodulate in-phase and quadrature tension components. The phase axis of demodulation was adjusted for zero output of the quadrature signal in rigor. The sinusoidal frequency was 500 Hz and the post-demodulation filter band width (3 dB point) was 30 Hz. Amplitude of the length oscillations was 1 μm peak-to-peak excursion at the piezoelectric stack end of the muscle fibre, resulting in a sinusoidal change in fibre length of less than 0·05 %.

---

to TF. Each end of the fibre was attached to a stainless-steel hook (SS), via epoxy-coated grass stems (GS1, GS2) cemented to FT and PS. *C*, arc-lamp radiation source. Light from the 200 W mercury arc was collected by a mirror (M) and transmitted through a quartz condensing lens (SL1). Light then passed through a water filter (WF), secondary focusing lens (SL2), electromagnetic shutter (S) and band-pass absorption filter (BPF; 300–400 nm). *D*, 347 nm laser light source. A ruby rod (RR) was optically pumped with light from a xenon flash lamp (not shown). The laser cavity was formed by the partially reflecting front face of RR and a rear reflector (RM). A Pockels cell (PC) and Brewster stack polarizer (BS1) formed a Q-switch to decrease the laser pulse duration to 50 ns. A small fraction of the energy was split from the main beam into a ballistic thermopile (BT) to monitor the energy produced by the pulse. A temperature-tuned RDA crystal acted as a frequency doubler to generate 347 nm radiation. A second Brewster stack (BS2) or blue filter (BF) eliminated 694 nm radiation. A quartz cylindrical lens (CL) focused the 347 nm light to the height of the trough (3 mm). A continuous helium–neon laser (HNL) was used to align the components of the ruby laser with the front trough containing the fibre. A microscope objective (MO) and a condenser (MC) were positioned in the vertical axis for measurements of sarcomere length and cross-sectional area.

This amplitude of oscillation had no appreciable effect on the steady tension or non-sinusoidal components of transient tension responses initiated by caged ATP photolysis.

Tension and stiffness were continuously recorded on a slow time base with a chart recorder, Gould 220, and during the photolysis trial on storage oscilloscopes (Tektronix, 5112) set at different sweep speeds. The oscilloscope traces were photographed on Polaroid (667) film. Tension and in-phase stiffness during the photolysis trials were also amplified (Pacific Instruments, model 3100), digitized at 12-bit, 0·1–1·0 ms resolution and stored on flexible diskettes by a Z80-based microcomputer. Timing pulses for the oscilloscopes, A/D converters, step length changes and the laser trigger were provided by a digital pulse generator (Devices Digitimer, 5134).

Synthesis and characterization of caged ATP

The synthesis of caged ATP was based on that of Kaplan *et al.* (1978). 1-(2-nitro)phenylethyl phosphate was prepared from its parent alcohol by the method of Khwaja, Reese & Stewart (1970). In the condensation step, 3 mmol 1-(2-nitro)phenylethyl phosphate was treated with 1 mmol ADP morpholidate in 12 ml dry dimethylsulphoxide for 20 h at 80 °C. Caged ATP was purified in three column chromatography steps. In the first and third steps caged ATP was chromatographed on diethylaminoethylcellulose (DEAE) with triethylammonium bicarbonate as eluting solvent. The second step involved high-performance liquid chromatography (h.p.l.c.) and was carried out in two batches on a C-18 column (25 cm × 2·5 cm diameter, Waters Associates) packed with 55–105 μm beads. The eluting solvent was 10 mM-KH_2PO_4 at pH 5·5 and methanol (85:15 v/v). Caged ATP was obtained in 30% yield from ADP morpholidate. The caged ATP was desalted by the third chromatography step and then stored in the dark at −20 °C as its triethylamine salt in water at neutral pH. The caged ATP stock solution (100 mM) contained less than 0·01% ATP. Caged ATP was characterized by h.p.l.c. on analytical C-18, NH_2-Bondapak and SAX columns (Waters Associates) with eluant monitoring at 260 nm and by its conversion to ATP on photolysis. Concentrations of caged ATP were determined from its absorption coefficient $\epsilon_{260\ nm} = 19{\cdot}6\ mM^{-1}\ cm^{-1}$. At 347 nm (the wave-length of the laser pulse) $\epsilon = 660\ M^{-1}\ cm^{-1}$.

Optical components

The light source for photolysis of caged ATP was either a 200 W mercury arc lamp or a frequency-doubled ruby laser. Radiation from the arc lamp was collimated by a 50 mm quartz condensing lens (SL1 in Fig. 1*C*). A 150 mm quartz secondary focusing lens (SL2) produced an expanded image of the arc at the muscle fibre. A mechanical shutter (S) (Vincent Associates, model 214-L) timed the irradiation of the muscle fibres and caged ATP solution. Wave-length selection was made by a 10 cm water filter (WF) and a 300–400 nm band-pass filter (BPF) (Oriel, 5181). The arc lamp illumination of caged ATP at an initial concentration of 2 mM resulted in a continuous liberation of ATP at about 300 $\mu M\ s^{-1}$ in the trough containing the fibre.

More intense and shorter pulses of 347 nm radiation could be focused on to the muscle fibre from the laser source as shown in Fig. 1*D*. The ruby laser (Control Laser, model 634) produced a 3–5 J pulse of light at 694 nm. A 13 × 160 nm ruby rod (RR) was water cooled to 18 °C and optically pumped by a helical xenon flash lamp. The resonant optical cavity of the laser laser consisted of the partially reflecting front surface of the ruby rod and a totally reflecting back mirror (RM). The resonance of this cavity was damped below the threshold for laser oscillation by a Pockels cell (PC; Inrad, 203–150) and vertically polarized Brewster stack (BS1). At the peak of the xenon lamp pulse a thyristor circuit rapidly reduced the (3 kV) Pockels cell voltage to zero, increasing the resonant quality (Q) of the cavity to above the threshold for laser oscillation. This Q-switched mode of operation (Yariv, 1975) reduced the pulse duration to ≈50 ns (full width at half-maximum intensity) so that the peak intensity was high enough (100–200 MW) for efficient frequency doubling. A sample (≈15%) of the primary laser beam was reflected by a glass slide on to a ballistic thermopile (BT) which monitored the intensity of each pulse.

The frequency doubler was a 25 mm crystal of rubidium dihydrogen arsenate (RDA; Inrad, 520–004) in a temperature-stabilized housing. The dielectric polarization of the RDA medium by the electric field of the fundamental 694 nm radiation is slightly non-linear, leading to propagation of radiation at the second harmonic, 347 nm. RDA has the same index of refraction at 694 and 347 nm when the temperature of the crystal is 101·2 °C. Thus, energy can propagate at both wave-lengths in constant phase relation leading to efficient energy coupling between the fundamental and second harmonic beams (Yariv, 1975). The polarization of the primary laser light was vertical

and polarization of the 347 nm beam was horizontal, so the primary beam could be attenuated to about 1% intensity by horizontally oriented quartz Brewster stacks (BS2). The efficiency of frequency doubling by the temperature-tuned RDA crystal was 3–10% so that up to about 300 mJ of energy at 347 nm was available. The light intensity was adjusted by altering the energy of the primary xenon pump flash or by placing filters (BF; Corning, 3051) or glass microscope slides in the beam path.

The collimated 347 nm beam generated by the laser was circular in cross-section, with a diameter of 12 mm. The beam was compressed in the vertical direction to the dimension of the muscle trough (3 mm) by a cylindrical quartz 120 mm lens (CL) placed 20 cm before the fibre. In the horizontal direction (along the fibre axis) the beam was cut to the size of the trough (8 mm) by masks on the cylindrical lens. Beam alignments were made using a continuous helium–neon laser (HNL) in the optical axis of the ruby laser and directed backwards through the fibre location. A fine check of alignment was made by placing a strip of unexposed, developed Polaroid film at the position of the muscle fibre and triggering the laser. A 'burn pattern' on the film indicated the position and approximate distribution of the laser energy.

Trough and solution exchange

A dual trough arrangement was constructed to facilitate fibre handling and solution exchange. The front trough (TF in Fig. 1*B*) had a quartz window (QW) on the side toward the incident radiation and a polished stainless-steel block (SB) in the back to reflect the radiation and to regulate the trough temperature. An ethanol/water mixture (EW) flowed through the steel block to set its temperature in the range 0–35 °C. The ends of the trough were Teflon strips (TS) cut with slots for the length and force transducer hooks. The bottom of the trough was made from a glass slide for microscope illumination. On the other side of the steel block a simpler back trough (TB) was milled into a Delrin block.

The solution exchange mechanism was designed and constructed in conjunction with Dr M. A. Ferenczi. A hydraulic piston (HP) lowered the trough, suspending the muscle fibre in air for a brief period (< 5 s) during a change of solution. After being lowered, the troughs and the cooling block travelled horizontally on a ball-bearing slide to position the alternate trough below the fibre. The piston then raised the troughs to immerse the fibre in a new solution. The solution in the front trough could also be changed by the following sequence: the trough was lowered; its contents were evacuated through a vacuum port (VP); it was refilled with the new solution from a Teflon cannula (TC); and then raised to re-immerse the fibre.

Solutions

The constituents of the solutions which bathed the fibres are listed in Table 1, except where noted otherwise. The concentrations of the solution constituents were calculated by a computer program which used affinity constants from the literature to solve the multiple binding equilibria of the components. Reagent grade $MgCl_2$, EGTA, KOH and HCl were obtained from Fisher Scientific Co. ATP (vanadium-free), creatine kinase (CK), creatine phosphate (CP), glutathione (reduced) (GSH), and *N*-Tris(hydroxymethyl) methyl-2-aminoethane sulphonicacid (TES) were obtained from Sigma Chemical Co.

Assay for ATP liberation

The rate constant of ATP release from caged ATP after absorption of a photon was inferred from the rate of the characteristic absorption change at 400 nm (McCray, Herbette, Kihara & Trentham, 1980). The rate constant was 118 s^{-1} in the caged ATP solution (see Table 1 for constituents) at pH 7·1 and 20 °C.

After photolysis, the contents of the muscle fibre trough were transferred by suction into small polypropylene vials, frozen and stored in the dark at −22 °C for subsequent ATP assay within 2–4 weeks. The concentration of ATP liberated by photolysis was determined in these samples with a luciferin–luciferase assay (McElroy & Strehler, 1949). Aliquots (3–5 μl) of the sample solution were mixed within 0·25 s with a large excess of a luciferin–luciferase solution. Each vial of luciferin–luciferase (Sigma, FLE-50) was made up to 20 ml with water and centrifuged at 4000 rev/min for 4 min to remove particulate matter. The supernatant was gently agitated in a darkened polypropylene beaker until required for the assay. Chemiluminescent light from the reaction of ATP with the luciferin–luciferase solution was monitored with a photometer constructed in the Johnson

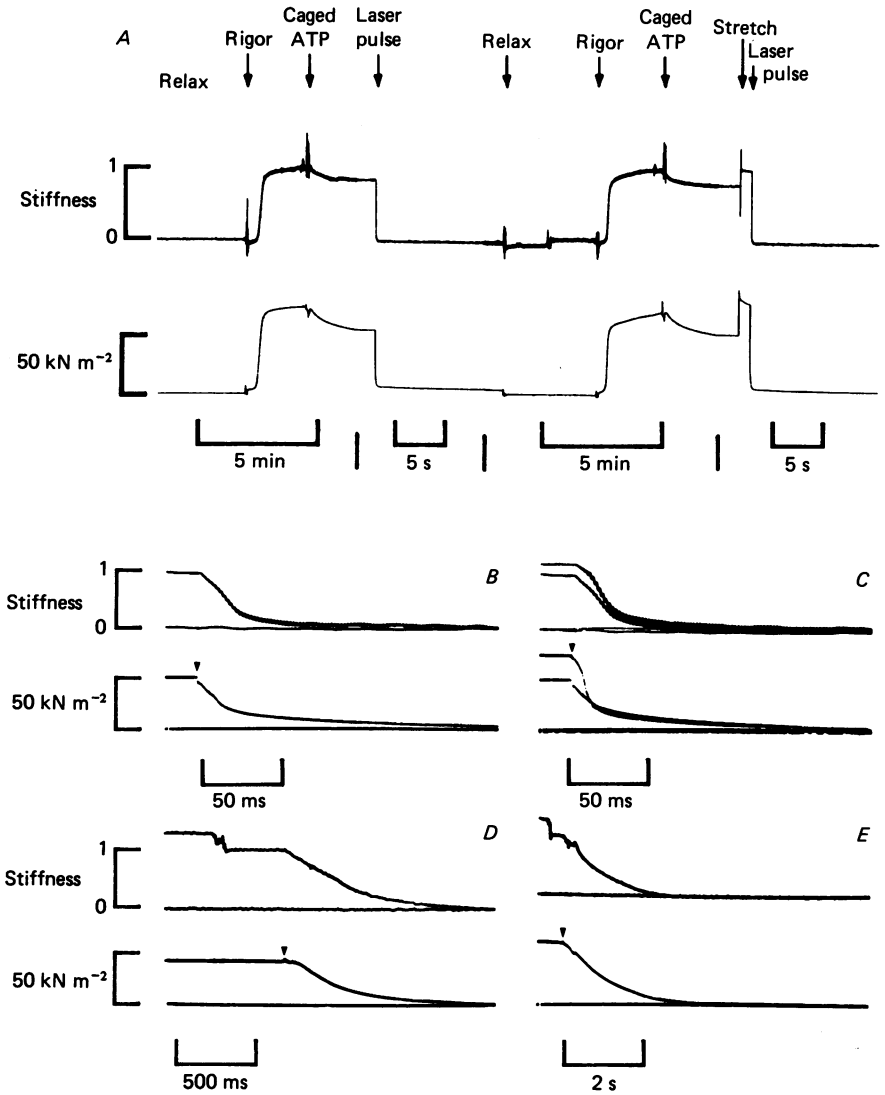

Fig. 2. Protocol for determining the mechanical properties of muscle fibres during relaxation from rigor. *A*, continuous chart recording of tension (lower) and in-phase stiffness (upper) from a single glycerol-extracted fibre. Arrows indicate timing of the solution exchanges, the laser pulses and a length change. Two successive rigor–photolysis–relaxation trials are illustrated. The length of the fibre was constant during the first trial. During the second rigor contraction a 0·53 % stretch was applied to the fibre 1 s before the laser pulse. Solution exchange was associated with artifacts in both tension and stiffness records (rapid vertical displacements of the record). Small changes in the base-line tension values at the time of solution exchange were due to surface tension on the force transducer pin (see Fig. 1, GS2). Note that the chart speed was increased before each laser pulse. The unit of stiffness calibration is the maximum rigor stiffness. Caged ATP concentration was 10 mM prior to photolysis. *B* and *C*, oscilloscope recordings of the relaxation phase of the trials illustrated in *A*. Arrow-heads mark the timing of the laser pulse. Photolysis yielded 594 μM-ATP. The flat traces show base-line tension and stiffness in the caged ATP solution 1 min after photolysis. In panel *C* the results from a pre-stretch

Foundation at the University of Pennsylvania. Typically, the light responses rose to a peak in about 1 s and then decayed over the next 30 s. Peak light intensity was used as an index of ATP concentration in the sample by calibration against standards which bracketed the sample ATP concentration. The assay was usually linear from 1 to 500 μM-ATP. Samples for sets of related experimental records were assayed with the same batch of luciferin–luciferase. The over-all variability of the assay was $\pm 5\%$, and two to four assays were performed from each test sample. 10 mM-caged ATP depressed the light response by approximately 10% at 1 mM-total ATP. The other constituents of the test solutions did not interfere with the assay for ATP release.

Since caged ATP absorbs light, the released ATP concentration is not constant across the 1·1 mm muscle trough. Estimates of the ATP gradient can be made from measurement of the light-intensity distribution in the laser beam and from the theoretical absorption of light by 10 mM-caged ATP. Assuming that ATP production is proportional to light intensity (McCray *et al.* 1980) and that the polished back surface of the trough reflects 50% of the light incident on it, the [ATP] at the muscle fibre, 0·55 mm from the front surface, would be 89% of the average [ATP] measured from the entire contents of the trough. The variation of [ATP] across a 100 μm muscle fibre should be about 12%. Non-uniformity of ATP production along the fibre length from uneven illumination is predicted to be maximally 30% but is usually less than 10%.

Experimental protocol

Tension and in-phase stiffness recordings during the solution exchange procedure (Fig. 2*A*) show the sequence of events in two rigor–photolysis trials. The muscle fibre was initially relaxed in 100 μM-Mg ATP in the back trough and was transferred to rigor solution (no CP, see Table 1) in the front trough (at the first arrow labelled 'Rigor'). Tension and stiffness increased, indicating rigor cross-bridge attachment. The solution in the front trough was exchanged for rigor solution with excess Mg^{2+} and 10 mM-caged ATP (at the arrow labelled 'Caged ATP'). 2 min were allowed for caged ATP to diffuse into the filament lattice. A laser pulse resulted in rapid relaxation of the fibre as shown in the faster time-base recording of tension and stiffness (panel *B*). Base-line force and stiffness levels were recorded and then the fibre was returned to the 100 μM-ATP relaxing solution in the back trough ('Relax'). The contents of the front trough were transferred to a sample vial for ATP assay. The front trough was cleaned with water and refilled with rigor solution.

Fig. 2*A* (right side) shows the next rigor–photolysis cycle conducted as described above, except that the fibre was stretched by 0·53% 1 s before the laser pulse. Note that the time base of the recording was expanded in this interval. The stretch led to an increase of rigor tension which remained elevated until the laser pulse was triggered. Panel *C* shows a rapid time base recording of relaxation after the pre-stretch, superimposed on the initial isometric photolysis trial.

Artifacts of the method

Some variability occurred in the magnitude of tension at the time of the laser pulse, even if the muscle fibre was held at a constant length. Tension occasionally decreased abruptly as the fibre was drawn through the air–solution interface. Some drop in rigor tension was typically noted as caged ATP diffused into the fibre. This latter effect seemed to be related to the particular batch of caged ATP and might indicate an impurity. If an impurity is present it is unlikely to be ATP or ADP as judged by h.p.l.c. analysis of the caged ATP stock or by the mechanical response of the muscle fibre (see Ferenczi, Homsher & Trentham (1984) for further discussion of this phenomenon). We did not observe any marked dependence of the mechanical transients on the magnitude of these artifacts.

Another artifact is illustrated in Fig. 3 (tension trace *a*). At the time of the laser pulse the rigor

---

trial (upper tension and stiffness records) are superimposed upon the isometric trial. The higher stiffness level can be attributed to the non-linear force extension curve of the fibre. *D* and *E*, oscilloscope records of relaxation induced when the same fibre was transferred from a rigor solution into relaxing solutions containing 5 mM- and 0·5 mM-Mg ATP respectively. Caged ATP was not present in these solutions. Arrows mark the time at which the fibre was placed into the relaxation solution. Earlier deflexions on the stiffness recordings occurred when the trough was lowered for the solution exchange. Sarcomere length = 2·45 μm; fibre dimensions: 3·12 mm × 5840 μm^2; T = 20·6 °C.

tension dropped immediately to 10% of its steady value. Tension then increased somewhat and finally decreased to the relaxed level. On the subsequent trial, the instantaneous drop of tension at the laser pulse (trace *b*) was much less and the final phase of relaxation followed a time course similar to the first trace. Trace *c* is a pre-stretch experiment which shows an altered initial phase of the relaxation, but the final relaxation is similar to the other two traces. Thus the immediate tension drop simulates a length change. The initial instantaneous drop in tension was present in

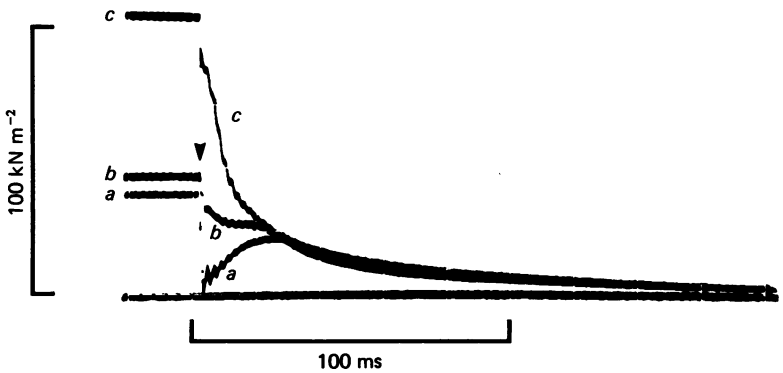

Fig. 3. Tension artifact during the initial photolysis trial. Tension recordings of relaxation from the first three rigor contractions obtained from the fibre are photographically superimposed. Trace *a*, first photolysis trial. The tension dropped to about 10% of the rigor tension during the first ms following the laser pulse. Trace *b*, second photolysis trial, in which over 80% of the initial tension remains after the first ms of the transient. The initial drop in tension illustrated by trace *a* is greatly reduced. Trace *c*, third photolysis trial obtained after a 0·66% pre-stretch. Tension base lines recorded after each trial are superimposed (lowest trace). Initial caged ATP concentration was 10 mM for each trial, and 400 μM-ATP was liberated by photolysis. The solution did not include CP or CK, but contained 2·5 mM-P^1,P^5-di(adenosine-5′-)pentaphosphate (Ap5A). Sarcomere length = 2·42 μm; fibre dimensions: 2·52 mm × 6652 μm^2; T = 19·6 °C.

most fibres in the first photolysis trial but varied in magnitude from 20 to 90% of the rigor tension. This artifact decreased or became negligible with the subsequent trials. Relaxations in which this large immediate tension drop occurred were not used for kinetic analysis.

In an initial series of experiments the muscle fibres failed to relax from rigor when caged ATP was photolysed by the arc lamp source. A control experiment was therefore performed in order to distinguish effects of the stable photoproduct from effects of the 347 nm light or from transient intermediates of the photochemical reaction (such as di-radicals). Fig. 4*A* is the tension record of a fibre put into rigor and then relaxed in 100 μM-Mg ATP. During the next rigor contraction (*B*) the fibre was immersed in a previously photolysed caged ATP solution with 180 μM-ATP and 180 μM-2-nitrosoacetophenone produced from 0·85 mM-caged ATP. Relaxation occurred as in panel *A* but the fibre contracted again after a 30 s exposure to this solution. In a solution without the photolysis by-product at this ATP concentration, the fibre would have remained relaxed. Another rigor contraction showed that the fibre no longer relaxed completely in 100 μM-Mg ATP (panel *C*) but did maintain relaxation in 5 mM-Mg ATP. The results suggest that the fibre is modified by the by-product of caged ATP photolysis, 2-nitrosoacetophenone, so that a higher ATP concentration is required for relaxation.

Inclusion of reduced glutathione (GSH) in the solutions protected the fibres from this desensitization to ATP, suggesting that the 2-nitrosoacetophenone attacks thiol groups on the contractile proteins (Kaplan *et al.* 1978; Goldman, Gutfreund, Hibberd, McCray & Trentham, 1982*a*). Also, 10 mM-GSH was more effective than 2 mM-GSH in protecting the muscle fibres. At 10 mM-GSH some slowing (15%) of the relaxation was observed after six to ten rigor–photolysis sequences, at which time the experiment was terminated. This may indicate a residual effect of the photolysis

by-product. Only data from fibres that showed less than 15% decrease in relaxation rate between the initial series of photolysis trials and a control series at the end of the experiment are considered in the Results section.

We tested whether or not caged ATP can diffuse freely into the fibre by loading the fibre with caged ATP and then replacing the external medium with paraffin oil, which is essentially transparent at 300–400 nm. Arc lamp illumination of the fibre in paraffin caused relaxation at a rate similar to that observed when photolysis was carried out in aqueous external medium. This experiment shows that ATP released within the fibre is sufficient for relaxation.

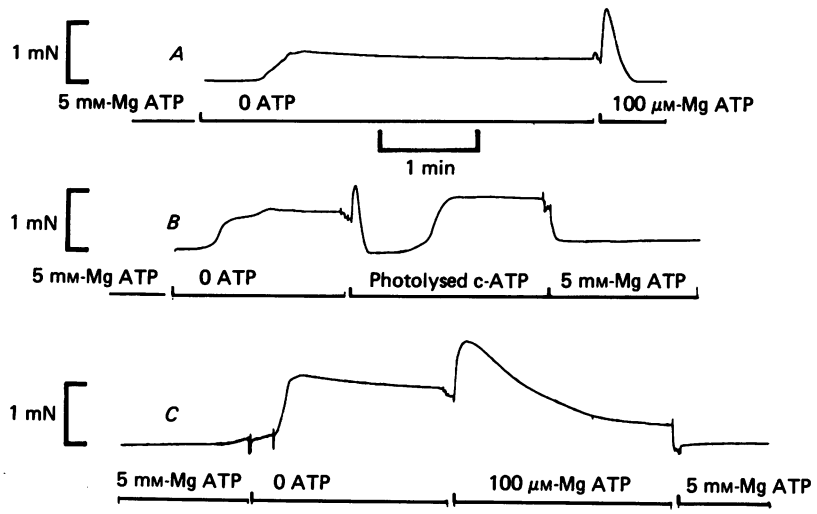

Fig. 4. Fibre modification by pre-photolysed caged ATP in the absence of glutathione. Successive recordings of isometric tension of a single fibre. Brackets mark the time of solution exchanges as labelled. An early prototype of the mechanical apparatus described in the text was used for this experiment. *A*, control rigor–relaxation cycle in glutathione-free solutions. *B*, relaxation from rigor initiated by immersing the fibre in a pre-photolysed caged ATP solution with 670 μM-caged ATP (c-ATP), 180 μM-ATP and 180 μM-2-nitrosoacetophenone produced by 1 s of arc lamp illumination. The fibre did not remain relaxed in this solution, and redeveloped force. *C*, subsequent rigor contraction. The fibre failed to relax fully when exposed to the 100 μM-Mg ATP relaxation solution used for trial *A*. $T = 23$ °C.

ATP-induced acto-subfragment 1 dissociation

For comparison with the muscle fibre experiments the kinetics of ATP-induced acto-subfragment 1 dissociation were measured at 22 °C in a stopped-flow spectrometer as described by Taylor & Weeds (1976). Some 5 μM-acto-subfragment 1 was mixed with 10–100 μM-Mg ATP in the rigor solution (Table 1) as solvent. Actin and subfragment 1 from rabbit skeletal muscle were prepared according to standard procedures (Lehrer & Kerwar, 1972; Weeds & Taylor, 1975). The rate of dissociation was proportional to ATP concentration, with a second-order rate constant of $3{\cdot}5 \times 10^6$ M^{-1} s^{-1}.

RESULTS

Improvement of time resolution

Fig. 2 shows a comparison between the rate of relaxation from rigor achieved with the pulse photolysis technique (panels *B* and *C*) and by diffusion of ATP into the filament lattice (*D* and *E*). For each panel, the fibre had been put into rigor and then

loaded with CP and CK for about 2 min before the oscilloscope sweep. In panels *B* and *C* caged ATP was included in the incubation medium and was photolysed as discussed above to produce 594 μM-ATP. In panel *D* the fibre was transferred to a relaxing solution with 5 mM-ATP, which diffused into the fibre during the recording.

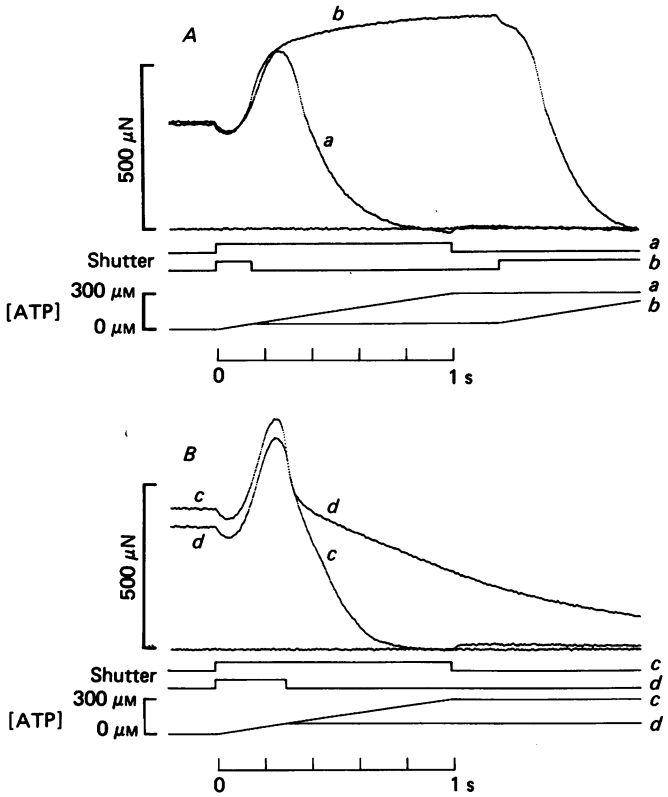

Fig. 5. Tension transients during slow liberation of ATP by arc lamp illumination. *a*, tension record in response to 1 s illumination of a solution with 2 mM initial caged ATP; 300 μM-ATP was formed during this period. The timing of the arc lamp illumination (shutter wave form) and calculated time course of released ATP concentration are also shown. *b*, following trial with a 150 ms photolysis period, followed by a 1 s dark period and then 600 ms illumination. *c*, tension recording with 1 s illumination period and production of 300 μM-ATP. *d*, tension response to 300 ms period of illumination releasing 155 μM-ATP. The flat traces indicate base-line tension. $T = 22$ °C. Lower vertical bar is released ATP concentration.

Panel *E* shows a similar diffusion-limited relaxation with 500 μM-ATP in the external medium. Note that the time base is slower for panels *D* and *E* compared to *B* and *C*. The half-time of relaxation using the pulse photolysis method is faster than that obtained by diffusing the same concentration of ATP into the filament lattice by a factor of about 50.

Arc lamp experiments

Fig. 5*A* shows tension from a fibre loaded with caged ATP at $< 10^{-8}$ M-free Ca^{2+} and then exposed to 1 s of illumination from the mercury arc lamp source (trace *a*). The

period of arc lamp illumination is indicated by shutter pulse *a*. The approximate time course of released ATP concentration in the trough is also shown. During the period of illumination the ATP concentration in the trough rose smoothly from <1 μM to 300 μM. Tension decreased slightly, increased to a peak, and then declined to the

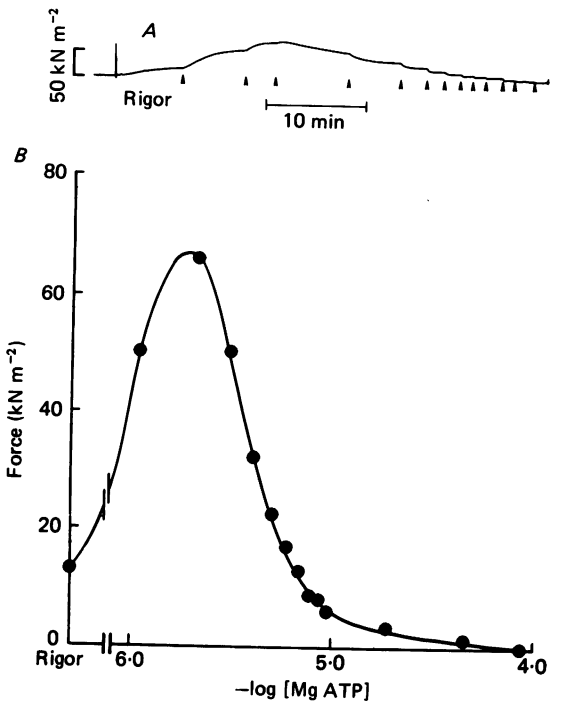

Fig. 6. Steady-state isometric tension *vs.* [Mg ATP] relation for a single muscle fibre. *A*, chart recording of tension during the removal and subsequent addition of ATP to the solution bathing the fibre. At the time of the tension artifact the fibre was transferred through an air interface into a trough containing rigor solution with CP and CK (Table 1). Arrows mark the times at which the ATP concentration was increased in steps by sequential addition of small volumes of a 0·1 or 1·0 mM-ATP relaxation solution (arrows). Several minutes were allowed for stabilization of tension at each Mg ATP concentration. *B*, tension *vs.* [Mg ATP] relation obtained from the recording in *A*. Each point on the plot corresponds to the final tension achieved at that Mg ATP concentration. Sarcomere length = 2·49 μm; fibre dimensions: 3·29 mm $\times$ 7311 μm^2; T = 19 °C.

relaxed level. The dependence of the tension rise on ATP formation was investigated by controlling the amount of ATP released. Trace *b* in Fig. 5*A* shows the tension during the next photolysis trial in which the shutter was closed during the rising phase of the transient. Tension rose to a relatively stable plateau above the rigor level. After a 1 s delay the shutter was opened again to resume photolysis. The tension then decreased monotonically to the relaxed level. The concentration of liberated ATP was calculated to be about 45 μM during the maintained plateau of tension.

Fig. 5*B* shows a comparison of tension records obtained with 1 and 0·3 s illumination periods (*c* and *d* respectively). An abrupt slowing in the rate of relaxation was observed in trace *d* when ATP formation was stopped. The final relaxation

occurred at a slower rate, presumably related to diffusion of ATP into the fibre from the external medium. These experiments show that with arc lamp illumination, the time course of the tension transient is critically dependent on continued production of ATP by photolysis.

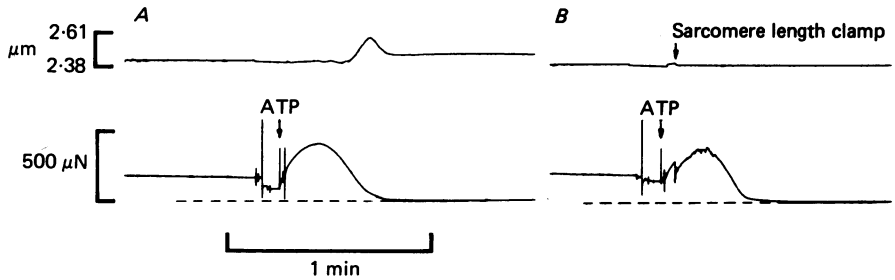

Fig. 7. Tension and sarcomere length transients during slow relaxation from rigor. *A*, sarcomere length (upper) and tension (lower) recordings of the change induced by the addition of 50 μM-Mg ATP to the solution in which the fibre was immersed. The fibre was held horizontally between a force transducer and a servo-controlled motor similar to that described by Ford *et al.* (1977). Sarcomere length signal (upper trace) was obtained by a white-light diffraction method (Goldman, 1983). At the beginning of the record the fibre was in rigor solution which was removed at the time marked by the large vertical artifact on the tension record. The fibre was immersed in a 50 μM-Mg ATP relaxation solution at the point marked 'ATP'. The dashed line has been added for clarification of the final relaxed tension level. *B*, repeat of the experiment illustrated in *A* but with the sarcomere length signal fed back to the servo-motor to clamp the sarcomere length at 2·4 μm. The sarcomere length feed-back was initiated at the time indicated by the arrow. Fibre dimensions: 2·70 mm × 5250 μm^2. The illuminated central segment was 1·8 mm long; $T = 21$ °C.

The effect of ATP concentration on steady-state tension could be shown more directly in an experiment in which a fibre was treated with fixed concentrations of ATP. Fig. 6*A* shows the isometric tension generated by a single fibre exposed to a series of increasing ATP concentrations in the presence of 1 mM-Mg^{2+} and $< 10^{-8}$ M-free Ca^{2+} ions and other solvent conditions as in the photolysis experiments (10 mM-GSH, ionic strength 200 mM). A biphasic curve of tension *vs.* Mg ATP concentration was obtained (Fig. 6*B*). Peak tension occurred at 1·81 ± 0·15 μM-Mg ATP (mean ± S.E. of mean, $n = 26$).

Length-clamp experiments

Non-uniformity of fibre compliance might lead to an early tension rise for the following reason. If ATP had induced shortening of the central section of the fibre, the compliance at the ends of the fibre would have been stretched, leading to an increase in the tension as observed in Fig. 5. A control experiment was conducted to test this possibility, with a length-clamp technique based on white-light diffraction (Goldman, 1983). Fig. 7 shows the tension and sarcomere length recordings from a central 1·8 mm section of a 2·7 mm fibre. Panel *A* shows the tension and sarcomere length changes when a fibre was put into rigor and then relaxed with 50 μM-Mg ATP in the external medium. Tension increased and then decreased, with a time course

presumably linked to ATP diffusion into the fibre. The striation spacing in the central segment of the fibre did not decrease appreciably during the phase of rising tension, although an elongation was observed during the final relaxation. The experiment was repeated (*B*), but in this case the striation spacing signal was fed back to a moving-coil motor (Ford, Huxley & Simmons, 1977) to clamp the sarcomere length constant in the central region. A similar tension response occurred.

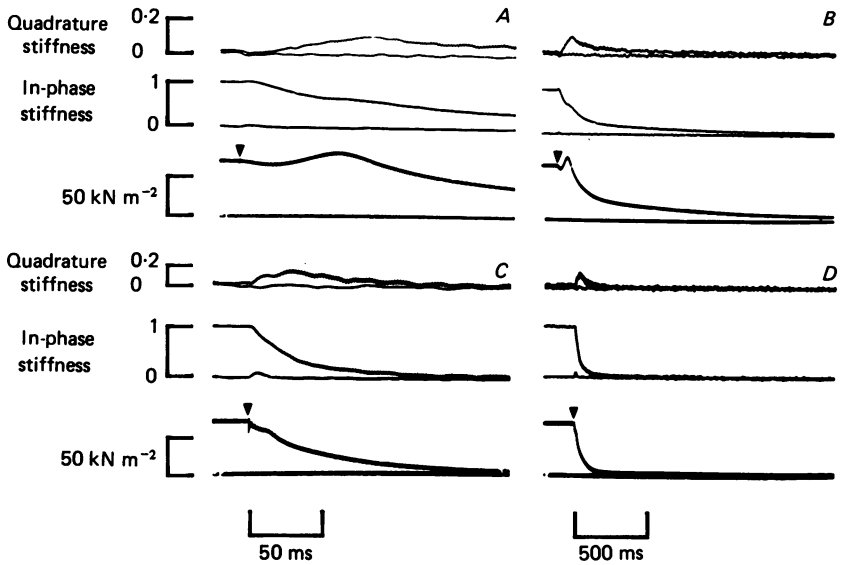

Fig. 8. Relaxation from rigor by laser photolysis of caged ATP. All panels show the transient changes in force (lower), in-phase stiffness (centre) and quadrature stiffness (upper) during the transition from rigor to the relaxed state. The frequency of the sinusoidal length change was 500 Hz, with an amplitude of 1 μm (0·033 %). Arrows mark the time at which the laser pulse initiated photolysis. The flat traces show base-line tension, in-phase stiffness and quadrature stiffness in the caged ATP solution about 1 min after relaxation. Left-hand panels (*A* and *C*) are fast time-base records; right-hand panels (*B* and *D*) are slower time-base records of the same events. The initial caged ATP concentration was 10 mM. *A* and *B*, liberation of 82 μM-ATP. Sarcomere length = 2·66 μm; fibre dimensions: 2·73 mm × 5081 μm^2; T = 20·3 °C. *C* and *D*, liberation of 348 μM-ATP. Sarcomere length = 2·51 μm; fibre dimensions: 2·98 mm × 4888 μm^2; T = 20·2 °C.

Although the transient tension rise and relaxation in this experiment were much slower than in a photolysis experiment, the qualitative nature of the processes was similar. The results indicated that a substantial shortening of the central region of the fibre was not required for a transient tension increase to occur.

Experiments with laser-induced photolysis

The 347 nm light pulse from the frequency-doubled laser was able to photolyse up to about 1 mM-caged ATP with a 50 ns light pulse. Better time resolution was available with this source, although release of ATP was limited to about 100 s^{-1} by the kinetics of the dark reactions following photon absorption (McCray *et al.* 1980). Fig. 8 shows representative records of tension, in-phase stiffness and out-of-phase

(quadrature) stiffness during relaxation initiated by laser photolysis of caged ATP in a rigor fibre. Base-line recordings of the tension and stiffness are also shown. Panels *A* and *B* are the same event recorded at two sweep speeds. Released ATP concentration was 82 μM. Panels *C* and *D* are a similar pair of recordings of a photolysis trial in a different fibre with 348 μM-ATP released.

After liberation of ATP the tension response had several phases. During the first 5–10 ms tension decreased. If the ATP concentration was below about 250 μM or the rigor tension was below about 50 kN m^{-2}, tension then increased (panels *A* and *B*). At higher ATP concentrations this second phase was apparent as a lag in the tension decay (panels *C* and *D*). Tension then decreased to the relaxed level, with a time course approximating the sum of two exponential components. At ATP concentration above 500 μM the apparent rate constants for the final relaxation were 110 ± 6 s^{-1} and $16{\cdot}5 \pm 0{\cdot}7$ s^{-1} (means $\pm$S.E. of means, $n = 24$). The amplitude of the faster component was 60 ± 5% of the amplitude of the slower final relaxation.

After the laser pulse, the in-phase stiffness decreased monotonically from the rigor level. The stiffness decrease was often delayed during the rising phase of the tension response (Fig. 8 *A* and *B*). The quadrature stiffness signal increased from its zero rigor level to a peak 20–40 ms after the tension rise and then decayed back to zero. The filtering of the quadrature signal necessary to extract it from the demodulator output truncated the peak of the recording by about 30%. The relative magnitudes of the two stiffness signals indicate that at the peak of the quadrature signal, the sinusoidal component of tension leads the length-driving wave form by $15{\cdot}9 \pm 0{\cdot}9$ deg (mean $\pm$S.E. of mean, $n = 13$) of phase shift at [ATP] $\approx$ 500 μM. A phase lead measured in the frequency range of 0·5 kHz is also a property of cross-bridges in active muscle contraction (Kawai & Brandt, 1980).

Stress dependence and the kinetics of cross-bridge detachment

Experiments were conducted to investigate how the kinetics of an ATP-induced relaxation were modified by the initial stress in the fibre. Rigor tension was perturbed by either a stretch or release of the fibre applied 1 s before the laser pulse. The time courses of the tension changes during the 20–40 ms following the laser pulse were markedly affected by the initial stress. The tensions then converged to the same value irrespective of the initial stress. The time courses of the remainder of the tension decays were the same and did not depend on the initial tension.

Fig. 9 shows two examples of superimposed records from pre-stretch (traces labelled s), isometric (i) and pre-release (r) trials. The manner in which the tension traces converged varied from fibre to fibre. In panel *A*, the pre-release trace (r_1) crossed over the two upper traces but then decayed more rapidly for about 20 ms, so that the tension during the final phase of relaxation was the same. Traces s, i and r_2 do not cross. In panel *B* the cross-over is more noticeable.

If some cross-bridges, detached by ATP, reattach to new actin sites during relaxation, the amount of force produced by the reattached cross-bridge may not depend on its original rigor stress. In that case, during the final relaxation, the tension derived solely from reattachments would be independent of the initial stress. Convergence of two traces which start at different tensions would then indicate the loss of the original stress difference, and this convergence would occur at the rate of the initial cross-bridge detachment.

Algebraic differences between pairs of tension traces were therefore calculated to measure the rate of the presumed initial detachment. This is illustrated below the original data in each panel of Fig. 9. Each difference trace reached a value near zero well before the over-all relaxation was complete. The convergence of the tension traces was slightly faster for the upper pair of traces than for the lower pairs. For a series

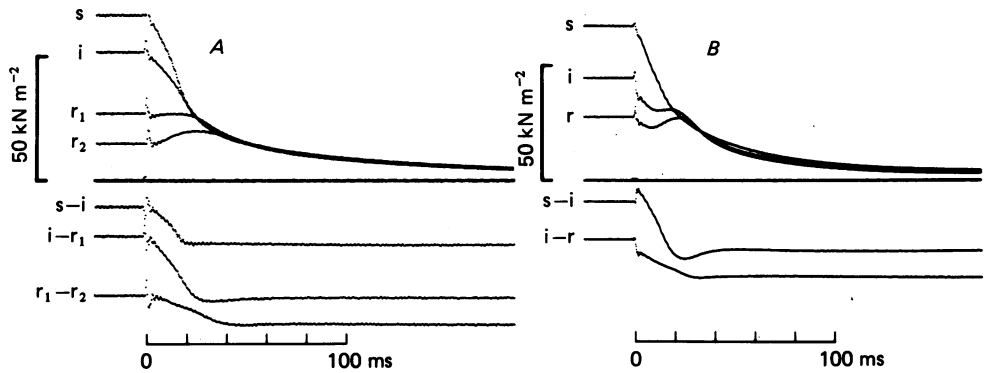

Fig. 9. Superimposed tension records from several successive rigor–photolysis trials in two different fibres (*A* and *B*). The upper set of records in each panel are original tension recordings, with tension base lines in the photolysed caged ATP solution about 1 min after relaxation. Records are labelled s (stretch), r (release), or i (isometric) according to the length change applied 1 s prior to photolysis. Algebraic differences between adjacent pairs of tension records are shown below the tension base line (e.g. s–i is the difference between original records s and i). Prior to photolysis, 10 mM-caged ATP was present in solutions. *A*, 557 μM-ATP was liberated by photolysis. Sarcomere length = 2·46 μm; fibre dimensions: 2·18 mm × 4719 μm^2; T = 20·4 °C. Length changes: s, 0·38 % stretch; r_1, 0·76 % release; r_2, 1·52 % release. *B*, 550 μM-ATP was liberated by caged ATP photolysis. The laser pulse was at time zero. Sarcomere length = 2·22 μm; fibre dimensions: 2·24 mm × 5386 μm^2; T = 22·8 °C. Length changes: s, 0·55 % stretch; r, 0·37 % release.

of fibres, the half-times for convergence of pairs of tension records averaging 80·8 ± 3·6 kN m^{-2} were 1·46 ± 0·05 times faster than for corresponding pairs of tension records averaging 56·7 ± 3·8 kN m^{-2} (means ± S.E. of means, n = 20). The cross-bridge stress had a small but significant effect on the detachment rate measured by this subtraction method. Cross-bridges with greater stress in rigor appear to detach somewhat more rapidly than more lightly loaded cross-bridges.

Dependence of cross-bridge detachment rate on ATP concentration

Based on the interpretation that convergence of the tension traces indicates initial cross-bridge detachment, the subtraction method was used to measure the rate of cross-bridge detachment as a function of ATP concentration. In the experimental records shown in Fig. 10, the released ATP concentration in different trials was altered by adjusting the intensity of the laser pulse. As the final ATP concentration was increased, the time to the peak of the tension rise decreased and the amplitude of the tension rise decreased. Similar results were obtained when the ATP concentration was altered by changing caged ATP concentration (data not shown). The rate constant for the final relaxation phase did not correlate with ATP concentration, although the faster tension decrease preceding final relaxation (panel *A*) was less

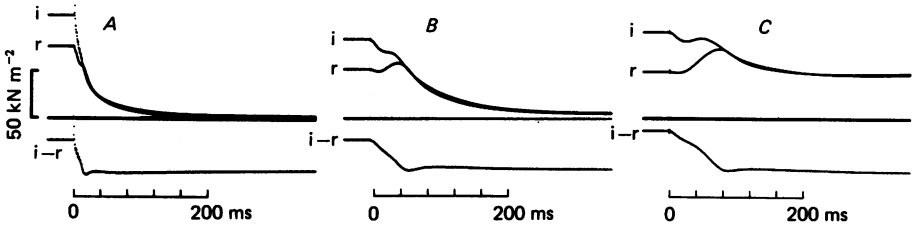

Fig. 10. ATP dependence of the convergence rate of tension records produced in pre-release and isometric photolysis trials. In each panel a pair of original tension records are shown from an isometric (i) trial and a trial after a 0·93 % release 1 s before the laser pulse (r). The flat traces are tension base lines. Algebraic difference records are shown below each pair. The caged ATP concentration was 10 mM prior to photolysis; the final ATP concentrations were: *A*, 512 μM; *B*, 233 μM; *C*, 106 μM. The laser pulse was at time zero. Sarcomere length = 2·54 μm; fibre dimensions: 2·67 mm × 4337 μm^2; T = 19·9 °C.

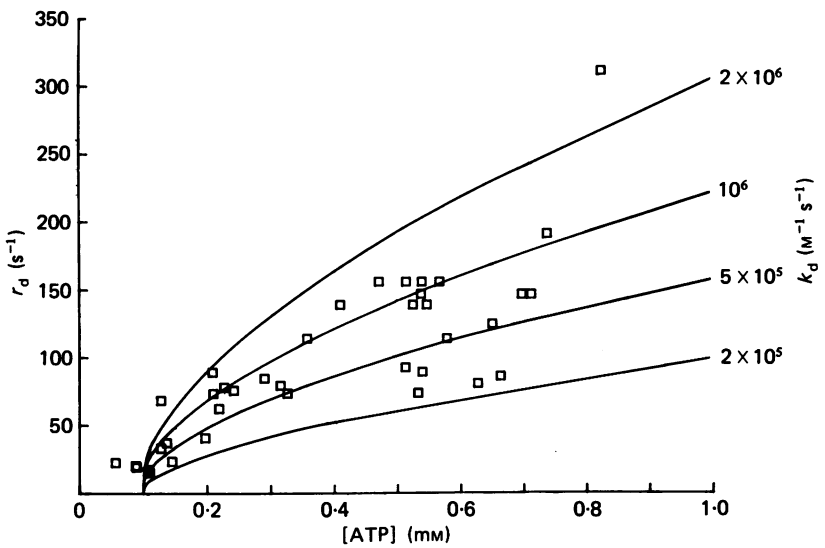

Fig. 11. Apparent rate of cross-bridge detachment from rigor as a function of ATP concentration. The detachment rate was estimated from the decay of the difference in tension arising from a 0·3–0·8 % pre-stretch or 0·3–1·5 % pre-release of the fibres 1 s before photolysis (see text for further explanation). The reciprocal of the half-time for the decay (r_d) is plotted on the ordinate, and the final ATP concentration produced by photolysis is plotted on the abscissa. The symbols represent the experimental data points obtained from thirty-eight pairs of trials in experiments with six single fibre segments. Since total ATP is plotted, the concentration of Mg ATP would be about 10 % lower. Another correction which could be applied to the data is the effect of caged ATP on the luciferin–luciferase ATP assay. The effect of this correction would be to shift the data points about 10 % higher along the abscissa. The lines represent the expected relation between r_d and [Mg ATP] determined from a computer simulation as described in the text. The equations were integrated using the Gear (1971) method. Diffusion of ATP into the fibre from the surrounding solution was not taken into account in the simulation.

prominent at lower ATP concentrations (panel *B*). At ATP concentrations below approximately 100 μM in the absence of CP and CK, the fibre failed to relax. However, tension traces still converged to a common time course. At each ATP concentration the isometric trials (traces i) showed less tension rise than the pre-release trials (r). Below each pair of tension records, the difference resulting from algebraic subtraction of the two traces is shown. The decay rate of the difference traces also depended on the final ATP concentration. Since the difference traces were not exponentials they were characterized by half-times ($t_{\frac{1}{2}}$) and plotted as reciprocal half-times ($r_d = 1/t_{\frac{1}{2}}$) against the ATP concentrations in Fig. 11.

The lines plotted in Fig. 11 are reciprocal half-times expected on the basis of the following sequence of reactions:

$$\text{Caged ATP} \xrightarrow{k_p} \text{ATP}$$

$$\text{ATP} + \text{AM} \xrightarrow{k_d} \text{M.ATP} + \text{A}$$

The curves have been drawn assuming that ATP was released from caged ATP after the laser pulse with a rate constant of (k_p =) 100 s^{-1} and that ATP bound to and detached rigor cross-bridges with a second-order rate constant of (k_d =) 2×10^5–2×10^6 M^{-1} s^{-1}. Myosin head concentration ([M]) within the fibre was assumed to be 200 μM. This value influences the expected half-time curve; at ATP concentrations less than 200 μM the above reaction sequence would not allow detachment of all the rigor cross-bridges and thus the traces would not converge. Experimentally the half-time for convergence of the traces can still be evaluated (e.g. Fig. 10*C*), hence there is necessarily divergence between the plotted lines and the data at low ATP concentrations. For [ATP] above 500 μM, the value assumed for [M] has little effect on the expected reciprocal half-time (15% decrease of $t_{\frac{1}{2}}$ as [M] is altered from 280 to 120 μM).

Recent studies have suggested that the photochemical dark reactions may be more complicated and that two processes contribute to the kinetics of ATP release. The first of these is the *aci*-nitro decay which occurs at (k_p =) 118 s^{-1} in the rigor solution. The second occurs at 64 s^{-1} and is inferred from measurements of the rate constant of release, k_q, of the photolysis by-product, 2-nitrosoacetophenone (J. A. McCray, H. Gutfreund & D. R. Trentham, personal communication). In this case $t_{\frac{1}{2}}$ will depend on three sequential processes, controlled by rate constants k_p, k_q and k_d[1].

Temperature dependence of relaxation kinetics

As expected, the over-all relaxation rate increased with temperature as did r_d ($= 1/t_{\frac{1}{2}}$) measured from tension difference records (Fig. 12). Q_{10} for r_d was $2{\cdot}7 \pm 0{\cdot}3$ ($n = 26$ subtraction traces) in the temperature range 10–20 °C. It should be noted that the Q_{10} for the rate of liberation of ATP from caged ATP is about 2·3 in this temperature range (J. A. McCray, H. Gutfreund & D. R. Trentham, personal communication). Thus the slowing at low temperatures may be partly related to slower ATP release. Q_{10} for the final phase of relaxation was 3·5. At 9·8 °C, pairs of tension traces starting at higher initial rigor levels converged earlier than those starting at lower rigor tension, as observed at 20–22 °C.

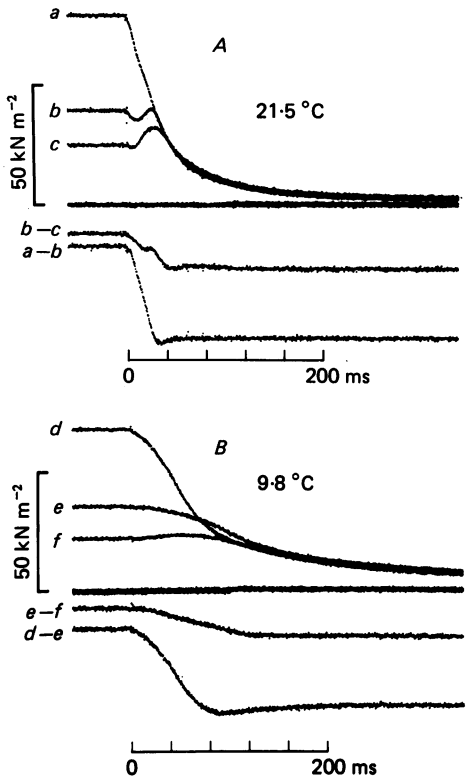

Fig. 12. The effect of temperature on relaxation and cross-bridge detachment. The caged ATP concentration was 5 mM prior to photolysis, and solution did not contain CP or CK. *A*, tension and algebraic difference records obtained from a single fibre at 21·5 °C. Final ATP concentration was 631 μM. *B*, tension and difference records obtained from the same fibre at 9·8 °C. Final ATP concentration was 442 μM. Traces *a* and *d* were isometric trials. Length changes applied 1 s before the laser pulse: *b* and *e*, 0·64 % release; *c* and *f*, 1·27 % release. The flat traces are tension base lines. The laser pulse was at time zero. Sarcomere length = 2·60 μm; fibre dimensions: 2·61 mm × 7526 μm^2.

An interesting feature of the tension records was that the amplitude of the transient tension rise following ATP release was greater at higher temperatures. This suggests that as the temperature is raised, the rate constant of the process controlling cross-bridge reattachment is increased relatively more than that controlling detachment.

DISCUSSION

Photolysis method

Photochemical generation of ATP greatly improves the time resolution for experimental determination of the rate of cross-bridge detachment (Fig. 2), although the kinetics of the dark reactions following photon absorption limit the precision of estimating the rate constants for detachment. Several requirements must be met by a photolabile precursor of a biologically active molecule for successful implementation of this photochemical method (Lester & Nerbonne, 1982). Caged ATP fulfils most of

these requirements, including high solubility and quantum yield in aqueous medium and a photolysis action spectrum in a wave-length range (310–360 nm) outside that of most protein absorption bands (Kaplan *et al.* 1978).

Binding of caged ATP to the ATPase active site of actomyosin has not been detected (McCray *et al.* 1980). In muscle fibres the rate of relaxation from rigor increased with ATP concentration regardless of whether the ATP release was increased by greater light intensity or by higher initial caged ATP concentration, indicating that binding of caged ATP to the ATPase active site on the cross-bridge was either weak or negligible. Some decrease of rigor tension usually occurred when caged ATP was included in the solutions (Fig. 2*A*). The possibility has not been ruled out that the tension decline is due to an impurity in the caged ATP stock solution or to the binding of caged ATP to locations other than the active site (Ferenczi *et al.* 1984). The presence of caged ATP in the filament lattice does not prevent either relaxation in the absence of Ca^{2+} or active contraction in the presence of Ca^{2+} (Goldman *et al.* 1982*b*; Hibberd, Goldman & Trentham, 1983; Goldman *et al.* 1984).

Several chemical changes associated with photolysis might influence the mechanical response of the fibre. The main by-product of photolysis of caged ATP is 2-nitrosoacetophenone. This compound forms an adduct with the thiol reagent dithioerythritol (Goldman *et al.* 1982*a*) and thus might attack thiol groups on myofibrillar proteins. Fig. 4 shows that the by-product of photolysis can alter the sensitivity of the muscle fibre to relaxation by ATP. Inclusion of 10 mM-reduced glutathione in the solutions was effective in maintaining fibre sensitivity to ATP, presumably by competing with protein thiol groups for the nitrosoketone. When caged ATP was photolysed by arc lamp illumination in red cell ghosts, the Na^+ pump was protected from irreversible modification by adding an amount of glutathione stoicheiometric with the 2-nitrosoacetophenone released (Kaplan *et al.* 1978). However, in the muscle fibre system a higher glutathione concentration was required for effective protection. Variable reactivity of protein thiols and sensitivity of proteins to thiol modification probably explain this difference.

The other by-product of the photochemical reaction is a mole of protons for every mole of ATP released (McCray *et al.* 1980). The physiological solutions used in this study were buffered with 100 mM-TES. Excess Mg^{2+} was present in all solutions. Any transient changes in the system arising from H^+ release and the equilibration of Mg^{2+} with ATP would be complete within 1 ms, based on the kinetics of H^+ and Mg^{2+} binding to amine buffers and ATP respectively (Diebler, Eigen & Hammes, 1960; Eigen, 1964). Thus the time course of cross-bridge detachment was unlikely to be influenced by transient changes in H^+ concentration or to be limited by Mg^{2+} binding to ATP.

Since some of the laser pulse energy absorbed in the trough was lost by thermal decay modes of the excited molecules, a temperature increase was expected at the start of photolysis. If all of the absorbed energy was lost as heat, the increase in temperature would have been 0·2 °C in a typical experiment. Based on the experiments in which the steady temperature was altered (Fig. 12), the small temperature jump would not appreciably modify the kinetics of cross-bridge detachment.

Transient tension increase

Evidence for transient reattachment of cross-bridges

A biphasic curve of steady tension *vs.* Mg ATP concentration (Fig. 6) in the absence of Ca^{2+} has been described previously by many authors (Reuben, Brandt, Berman & Grundfest, 1971; Fabiato & Fabiato, 1975; Arata, Mukohata & Tonomura, 1977). The generally accepted explanation of this curve is that cross-bridge cycling occurs at low ATP concentration even in the virtual absence of Ca^{2+}, because attached rigor links (actomyosin with no bound nucleotide) remove tropomyosin inhibition of cross-bridge attachment (Bremel & Weber, 1972). In addition there is evidence that cross-bridge cycling (attachment and detachment) apparently occurs in the range of 1–30 μM-Mg ATP ($[Ca^{2+}] < 10^{-8}$ M) since the ATPase activity is relatively high (Arata *et al.* 1977) and muscle fibres actively shorten and redevelop tension after a length release (Kawai & Brandt, 1976).

In the photolysis experiment of Fig. 5, interruption of the illumination slowed or halted relaxation. Closing the shutter during the time course of the tension rise stopped any further increase of ATP concentration, causing tension to remain at the peak of the steady curve (Fig. 5*A*, trace *b*). Thus the phenomenon which explains the steady relation between tension and [Mg ATP] (removal of inhibition by rigor links: Bremel & Weber, 1972; Bremel, Murray & Weber, 1973) also underlies the transient rise in tension.

The calculated concentration ($\approx$45 μM) of liberated ATP during the maintained high tension state in Fig. 5 was higher than the ATP concentration ($\approx$2 μM) leading to maximal steady tension. This difference might be due to ATP binding by the cross-bridges so that the free ATP concentration in the fibre was lower than in the external medium. Further diffusion of ATP into the fibre occurred relatively slowly (Figs. 2*D* and *E* and 5*B*).

Analysis of the response of the fibre to sinusoidal length changes after release of ATP also indicates the presence of active cross-bridges. The sinusoidal tension response briefly develops a phase lead (positive quadrature signal) during the tension increase, and then decays to the relaxed level (Fig. 8). During active contractions the phase lead is maintained (Goldman *et al.* 1984). This type of phase lead in the frequency domain corresponds to the quick recovery of tension that occurs in an active contraction after a rapid length step in the time domain (Kawai & Brandt, 1980). A. F. Huxley & Simmons (1971) discussed evidence that the quick tension recovery after a step length change is an indication of the structural change in the cross-bridge which leads to the force-generating state (the power stroke). The quick recovery and sinusoidal phase lead are properties of actively force-generating cross-bridges rather than rigor attachments (Kawai & Brandt, 1980).

The records of Fig. 8 show that the in-phase stiffness of a muscle fibre decreases while the tension is increasing. If the stiffness per attached cross-bridge is independent of the state of the cross-bridge, the stiffness records are a semiquantitative indication of the number of attachments. A decreasing number of cross-bridges during the tension rise implies that the tension per cross-bridge is increasing. This result suggests that some detached cross-bridges reattach and produce active force.

Several possible artifacts of the sinusoidal stiffness method should be considered.

Non-linearity of end compliance tends to raise the apparent stiffness at higher tensions when the muscle fibre is stretched (Fig. 2*A*, right side; see also Goldman *et al.* 1984). During the transient tension rise after ATP release the non-linearity of compliance would raise the stiffness trace. Therefore a drop of measured stiffness during the tension rise is not accounted for by this type of non-linearity. On the other hand, the delay of stiffness decrease seen in Fig. 8*A* and *B* about 50 ms after the laser pulse might be an artifact due to non-linear end compliance.

The finite response time of the tension transducer reduces the amplitude of the stiffness traces. However, the method of demodulating the tension along a fixed phase reference axis causes this proportion to be constant so that it does not influence the shape of the stiffness traces. Tension recovery during the time course of the sinusoidal length changes would also truncate the response. This factor can be evaluated from the tension signal phase shift given by θ = arctan (quadrature signal/in-phase signal). The peak phase lead in the tension signal was typically (θ =) 16 deg. If the phase lead is caused by a first-order stress-relaxation, truncation of the in-phase signal would be approximately 7%. Larger truncations could occur if the quick phase recovery were markedly non-exponential.

The propagation time of the length change along the fibre introduces a phase shift into the sinusoidal tension response (Schoenberg, Wells & Podolsky, 1974). The observed decrease of in-phase stiffness might cause an increase in the propagation time, introducing a phase lag in the tension response. Thus the observed phase lead cannot be the result of an alteration of propagation time. A more detailed analysis of the two stiffness signals would require quantitative evaluation of the contributions from possible artifacts. However, these considerations indicate that the decrease of in-phase stiffness and the development of a phase lead during the tension rise are not primarily due to difficulties associated with the recording method.

The in-phase and quadrature stiffness signals suggest that cross-bridges present during the transient tension increase have two properties of active cross-bridges: quick recovery and high force. These observations strongly support the hypothesis that after being detached by ATP some cross-bridges reattach briefly and produce active tension before final relaxation.

Other possible explanations of the transient tension rise

(*a*) *Possible tension artifacts.* The tension rise is related to ATP formation rather than to other processes accompanying photolysis because liberation of ADP from caged ADP caused no such rise unless CP and CK were included in the medium (Goldman *et al.* 1982*b*). An artifact which might lead to a transient rise in tension is non-uniformity of mechanical compliance. However, control experiments under length-clamped conditions showed that when the end compliance is effectively eliminated a tension rise can occur (Fig. 7). We conclude that the tension rise is unlikely to be an artifact of the method.

(*b*) *Force-generating AM.ATP state.* If AM.ATP generates more force than AM, increasing Mg ATP concentration should cause an increase in the amplitude of the tension rise, contrary to the observation that increasing [Mg ATP] decreases the amplitude (Figs. 8 and 10; Goldman *et al.* 1982*b*). In isometric conditions at greater than 500 μM-liberated ATP the tension did not rise above the rigor level. Since

stiffness decreases during the rise in tension, a postulated high force AM.ATP state would require lower stiffness per cross-bridge than the rigor attachment (AM).

Moreover, a rapid decrease in the tension records within 5 ms of the laser pulse (Figs. 5, 8, 9, 10 and 12) can be explained by an initial detachment. This point is made more quantitative in the following paper (Goldman *et al.* 1984). These results suggest that AM.ATP is either short-lived or does not exert force higher than AM.

(*c*) *Faster detachment of negatively strained cross-bridges.* Since the characteristic periodicities of the thick and thin filaments differ (H. E. Huxley & Brown, 1967), attached rigor cross-bridges probably have a distribution of distortions. Forces in the attached cross-bridges may vary from high values pulling in the normal sliding direction to negatively strained attachments pushing the filaments in the direction of muscle elongation. If cross-bridges exerting negative force detach more rapidly than normally strained attachments when ATP is liberated in the fibre, the result would be an increase in force and a decrease in stiffness as observed. However, stretching the muscle fibre caused an increase in the apparent rate of detachment by ATP (Figs. 9 and 12). This effect is opposite to that required if negatively strained rigor cross-bridges detach more rapidly than cross-bridges bearing positive force.

While these arguments do not rule out contribution from a high force AM.ATP state and rapid detachment of negatively strained cross-bridges, they do suggest that the overriding effect which causes the tension rise is force generation by newly formed cross-bridges.

Events during a photolysis trial

A simple hypothesis for the sequence of events occurring after absorption of photons by caged ATP explains many features of the observed mechanical transients. After several milliseconds ATP is released and cross-bridge detachment begins. If the muscle has been pre-stretched, the tension decays faster than in an isometric trial because the increased rigor tension leads to a greater tension decrement per detachment. Some of the detached cross-bridges reattach and produce force as in an active contraction. This reattachment either increases tension or delays relaxation. Myosin heads are allowed to reattach in the absence of Ca^{2+} by co-operativity of the type observed in the ATPase of myofibrils: remaining cross-bridges relieve tropomyosin inhibition. Co-operativity between the two myosin heads might also contribute to reattachment. Since only a proportion of cross-bridges reattach, a net detachment occurs throughout the transient, and stiffness continuously decays. When too few attachments remain, the thin-filament regulatory system prevents reattachment and final relaxation occurs. At high initial rigor tensions the decrease in force due to detachments dominates the observed tension, so no rise occurs. However, the number of reattached cross-bridges does not markedly depend on the initial rigor tension, since transients superimpose during final relaxation. At low [Mg ATP], detachment is slower relative to reattachment. Therefore a higher proportion of myosin heads reattach to actin. At low [Mg ATP] reattached cross-bridges probably maintain attachment for a longer period than at high [Mg ATP], since the rapid phase of relaxation after the tension rise is not observed at low [Mg ATP]. Both of these effects accentuate the tension rise at low [Mg ATP]; see Figs. 5, 8 and 10 and section *Experiments with laser-induced photolysis.*

Rate of cross-bridge detachment

The observation that traces starting at different rigor tension levels converge and then superimpose for the remainder of the relaxation (Figs. 2, 9, 10 and 12), suggests that the force of a reattached cross-bridge is independent of its strain before it had detached. If cross-bridges retain the distortion introduced by a length change only as long as they remain continuously attached, convergence of the tension trace in pre-stretch and pre-release experiments indicates the rate of the first detachment of the rigor cross-bridges. Further support for this assumption obtained by a different method of analysis is discussed by Goldman *et al.* (1984).

The rate of convergence, measured as the reciprocal of the half-time (r_d) of the difference between two records starting at different rigor tensions, is roughly proportional to the final [Mg ATP] (Figs. 10 and 11). The lines plotted in Fig. 11 are reciprocal half-times expected on the basis of second-order rate constants for the reaction of ATP binding and detaching AM in the range of 2×10^5–2×10^6 M^{-1} s^{-1}. The expected reciprocal half-times are not directly proportional to [ATP] for several reasons. The plotted lines take into account the substantial myosin head concentration ([M]) in the fibre. At low nucleotide concentrations, free [ATP] markedly decreases during the transient as ATP binds to cross-bridges; therefore, the lines curve downward at low [ATP]. The lines in Fig. 11 also take into account the photolysis dark reactions which limit the rate of ATP release after caged ATP absorbs a photon. The value (100 s^{-1}) taken for the rate constant controlling ATP release is in the same range as the rate of the observed tension convergence. When final [Mg ATP] is substantially greater than [M], the photolysis dark reactions partially influence observed rates of detachment. However, we can estimate the second-order rate constant even though the dark reactions are relatively slow (Fig. 11). The data are clustered between the lines plotted for second-order detachment rate constants of 5×10^5 and 10^6 M^{-1} s^{-1}.

Goldman *et al.* (1982*b*) estimated a lower limit for the cross-bridge detachment rate of 2×10^5 M^{-1} s^{-1} from the half-time of the final tension relaxation phases after ATP release. In the present analysis the first detachment is isolated from subsequent and slower cycling. The present estimates take into account the rate of ATP release and the decrease in free [Mg ATP] expected during the transient because ATP binds to AM. Both of these effects tend to slow the observed tension relaxation, so the values for the initial cross-bridge detachment rate are higher than the rate of over-all relaxation. The subtraction traces indicating cross-bridge detachment are markedly non-exponential (Figs. 9 and 12), suggesting that the present characterization by a half-time is still not a complete description of ATP-induced detachment.

A comparison can be made of ATP-induced cross-bridge detachment in the fibres and ATP-induced actomyosin dissociation in solution. In the solvent conditions of the present experiments, actomyosin dissociation induced by ATP occurs at $3{\cdot}5 \times 10^6$ M^{-1} s^{-1}. Thus the rate of ATP binding and cross-bridge detachment is very similar in the filament lattice to that in solution. The arrangement of the proteins within the filaments, organization of the filaments into a lattice and the resulting decrease in mobility do not appear to exert a major influence on the rate of detachment by ATP. The photolysis dark reactions preceding ATP release limit the

rate of the transients to some extent, so it should be noted that cross-bridge stress might have more effect on detachment rate than is observed in the experiments (Fig. 9).

No evidence was obtained for saturation of the cross-bridge detachment rate at ATP concentrations up to about 800 μM. Thus, in a physiologically active contraction, when the cross-bridge reaches the AM state with no bound nucleotide (rigor state), ATP will bind and induce detachment within a few milliseconds. This conclusion depends on the assumption that the AM state of rigor achieved by removing ATP from the bathing medium is the same as the nucleotide-free cross-bridge state in a contraction. A possibility which should not be ignored is that in the active cycle there might be a longer-lived AM cross-bridge state which does not bind ATP and occurs before the rigor configuration. However, stretching the muscle fibre in rigor so that total force was in the range of an active contraction caused an increase in the detachment rate. This result makes it less likely that a hypothetical AM state is a heavily populated and force-generating intermediate.

When a rigor cross-bridge bears high force, the equilibrium between attachment and detachment should be shifted in the direction of lower probability of attachment (Hill, 1974). The increase in detachment rate observed for stretched muscle fibres may contribute to this change in the equilibrium constant. The experimental value measured for stress dependence of the cross-bridge detachment rate may be an underestimate because the photochemical dark reactions of caged ATP partially limit the rate of the observed mechanical transients.

The over-all ATP hydrolysis rate in active fibres occurs at about 1 s^{-1} (Curtin, Gilbert, Kretzschmar & Wilkie, 1974; Levy, Umazumi & Kushmerick, 1976; Takashi & Putnam, 1979; Ferenczi *et al.* 1984). Assuming that the cross-bridge cycle occurs at the rate of ATP hydrolysis, our results indicate that cycling cross-bridges spend less than 1 % of the time in the AM state.

In A. F. Huxley's (1957) cross-bridge model the detachment rate was made dependent on the cross-bridge force or distortion to explain the extra energy liberation when an active muscle shortens. We observed an influence of stress or strain on detachment as indicated by decay of the tension difference traces (Figs. 9 and 12). When the rigor tension was low, detachment was slower. The direction of this effect is opposite to that expected from Huxley's (1957) theory. However, since the detachment from the AM state is rapid compared to the cross-bridge cycle time, detachment from AM is not expected to control the cross-bridge cycle. If a slower step is accelerated at low or negative tensions, then our experiments suggest that this step is between cross-bridge attachment and AM.

[1] *Note added in proof.* It has now been shown (J. A. McCray & D. R. Trentham, personal communication) that this second process (controlled by k_q, p. 595) occurs subsequent to ATP release and is related solely to 2-nitrosoacetophenone formation. ATP release is controlled exclusively by the process with rate constant k_p as originally proposed by McCray *et al.* (1980).

We are grateful to Ms Jody Dantzig for expert assistance and helpful discussions, Mr Miles J. Gessow and Mrs Fanny Itshak for skilled technical assistance and Mrs Joan Loepp for preparation of the manuscript. The work was supported by grants from the NIH (HL15835 to the Pennsylvania Muscle Institute, and AM00745). M.G.H. was a fellow of the Muscular Dystrophy Association of America.

REFERENCES

ARATA, T., MUKOHATA, Y. & TONOMURA, Y. (1977). Structure and function of the two heads of the myosin molecule. VI. ATP hydrolysis, shortening, and tension development of myofibrils. *Journal of Biochemistry* **82**, 801–812.

BREMEL, R. D., MURRAY, J. M. & WEBER, A. (1973). Manifestations of cooperative behavior in the regulated actin filament during actin-activated ATP hydrolysis in the presence of calcium. *Cold Spring Harbor Symposia on Quantitative Biology* **37**, 267–275.

BREMEL, R. D. & WEBER, A. (1972). Cooperation within actin filament in vertebrate skeletal muscle. *Nature, New Biology* **238**, 97–101.

CURTIN, N. A., GILBERT, C., KRETZSCHMAR, K. M. & WILKIE, D. R. (1974). The effect of the performance of work on total energy output and metabolism during muscular contraction. *Journal of Physiology* **238**, 455–472.

DIEBLER, VON H., EIGEN, M. & HAMMES, G. G. (1960). Relaxations-spektrometrische Untersuchungen schneller Reactionen von ATP in wässeriger Lösung. *Zeitschrift für Naturforschung* **15b**, 554–560.

EASTWOOD, A. B., WOOD, D. S., BOCK, K. L. & SORENSON, M. M. (1979). Chemically skinned mammalian skeletal muscle. I. The structure of skinned rabbit psoas. *Tissue and Cell* **11**, 553–566.

EIGEN, M. (1964). Proton transfer, acid–base catalysis, and enzyme hydrolysis. Part I: elementary processes. *Angewandte Chemie* **3**, 1–19.

FABIATO, A. & FABIATO, F. (1975). Effects of magnesium on contractile activation of skinned cardiac cells. *Journal of Physiology* **249**, 497–517.

FERENCZI, M. A., HOMSHER, E. & TRENTHAM, D. R. (1984). The kinetics of magnesium adenosine triphosphate cleavage in skinned muscle fibres of the rabbit. *Journal of Physiology* **352**, 575–599,

FORD, L. E., HUXLEY, A. F. & SIMMONS, R. M. (1977). Tension responses to sudden length change in stimulated frog muscle fibres near slack length. *Journal of Physiology* **269**, 441–515.

GEAR, C. W. (1971). *Numerical Initial Value Problems in Ordinary Differential Equations*, chap. 11. New Jersey: Prentice-Hall.

GOLDMAN, Y. E. (1983). The relationship between force and velocity of sarcomere shortening measured by white light diffraction. *Biophysical Journal* **41**, 257a.

GOLDMAN, Y. E., GUTFREUND, H., HIBBERD, M. G., MCCRAY, J. A. & TRENTHAM, D. R. (1982*a*). The role of thiols in caged ATP studies and their use in measurement of the photolysis kinetics of *o*-nitrobenzyl compounds. *Biophysical Journal* **37**, 125a.

GOLDMAN, Y. E., HIBBERD, M. G., MCCRAY, J. A. & TRENTHAM, D. R. (1982*b*). Relaxation of muscle fibres by photolysis of caged ATP. *Nature* **300**, 701–705.

GOLDMAN, Y. E., HIBBERD, M. G. & TRENTHAM, D. R. (1984). Initiation of active contraction by photogeneration of adenosine-5′-triphosphate in rabbit psoas muscle fibres. *Journal of Physiology* **354**, 605–624.

GOLDMAN, Y. E. & SIMMONS, R. M. (1984). Control of sarcomere length in skinned muscle fibres of *Rana temporaria* during mechanical transients. *Journal of Physiology* **350**, 497–518.

HIBBERD, M. G., GOLDMAN, Y. E. & TRENTHAM, D. R. (1983). The mechanical response of muscle fibers to a rapid increase in concentration of ATP. In *Biological Structures and Coupled Flows*, ed. OPLATKA, A. & BALABAN, M., pp. 223–238. New York: Academic Press.

HILL, T. L. (1974). Theoretical formalism for the sliding filament model of contraction of striated muscle. *Progress in Biophysics and Molecular Biology* **28**, 267–340.

HUXLEY, A. F. (1957). Muscle structure and theories of contraction. *Progress in Biophysics and Biophysical Chemistry* **7**, 255–318.

HUXLEY, A. F. (1974). Muscular contraction. *Journal of Physiology* **243**, 1–43.

HUXLEY, A. F. & SIMMONS, R. M. (1971). Proposed mechanism of force generation in striated muscle. *Nature* **233**, 533–538.

HUXLEY, H. E. & BROWN, W. (1967). The low-angle X-ray diagram of vertebrate striated muscle and its behaviour during contraction and rigor. *Journal of Molecular Biology* **30**, 383–434.

KAPLAN, J. H., FORBUSH III, B. & HOFFMAN, J. F. (1978). Rapid photolytic release of adenosine 5′-triphosphate from a protected analogue: utilization by the Na:K pump of human red blood cell ghosts. *Biochemistry* **17**, 1929–1935.

KAWAI, M. & BRANDT, P. W. (1976). Two rigor states in skinned crayfish single muscle fibers. *Journal of General Physiology* **68**, 267–280.

KAWAI, M. & BRANDT, P. W. (1980). Sinusoidal analysis: a high resolution method for correlating biochemical reactions with physiological processes in activated skeletal muscles of rabbit, frog and crayfish. *Journal of Muscle Research and Cell Motility* **1**, 279–303.

KHWAJA, T. A., REESE, C. B. & STEWART, J. C. M. (1970). A convenient general procedure for the conversion of alcohols into their monophosphate esters. *Journal of the Chemical Society* (C), 2092–2100.

LEHRER, S. S. & KERWAR, G. (1972). Intrinsic fluorescence of actin. *Biochemistry* **11**, 1211–1217.

LESTER, H. A. & NERBONNE, J. M. (1982). Physiological and pharmacological manipulations with light flashes. *Annual Review of Biophysics and Bioengineering* **11**, 151–175.

LEVY, R. M., UMAZUME, Y. & KUSHMERICK, M. J. (1976). Ca^{2+} dependence of tension and ADP production in segments of chemically skinned muscle fibers. *Biochimica et biophysica acta* **430**, 352–365.

MCCRAY, J. A., HERBETTE, L., KIHARA, T. & TRENTHAM, D. R. (1980). A new approach to time-resolved studies of ATP-requiring biological systems: laser flash photolysis of caged ATP. *Proceedings of the National Academy of Sciences of the U.S.A.* **77**, 7237–7241.

MCELROY, W. D. & STREHLER, B. L. (1949). Factors influencing the response of the bioluminescent reaction to adenosine triphosphate. *Archives of Biochemistry* **22**, 420–433.

NATORI, R. (1954). The preparation and contraction process of isolated myofibrils. *Jikei Medical Journal* **1**, 119–126.

REUBEN, J. P., BRANDT, P. W., BERMAN, M. & GRUNDFEST, H. (1971). Regulation of tension in the skinned crayfish muscle fiber. I. Contraction and relaxation in the absence of Ca (pCa > 9). *Journal of General Physiology* **57**, 385–407.

SCHOENBERG, M., WELLS, J. B. & PODOLSKY, R. J. (1974). Muscle compliance and the longitudinal transmission of mechanical impulses. *Journal of General Physiology* **64**, 623–642.

SCHWARTZ, M. (1959). *Information Transmission, Modulation, and Noise*, chap. 4. New York: McGraw-Hill.

TAKASHI, R. & PUTNAM, S. (1979). A fluorimetric method for continuously assaying ATPase: application to small specimens of glycerol-extracted muscle fibers. *Analytical Biochemistry* **92**, 375–382.

TAYLOR, R. S. & WEEDS, A. G. (1976). The magnesium-ion-dependent adenosine triphosphatase of bovine cardiac myosin and its subfragment-1. *Biochemical Journal* **159**, 301–315.

WEEDS, A. G. & TAYLOR, R. S. (1975). Separation of subfragment-1 isoenzymes from rabbit skeletal muscle myosin. *Nature* **257**, 54–56.

WHITE, H. D. & TAYLOR, E. W. (1976). Energetics and mechanism of actomyosin adenosine triphosphatase. *Biochemistry* **15**, 5818–5826.

YARIV, A. (1975). *Quantum Electronics*. New York: Wiley.